Journal Pre-proofs

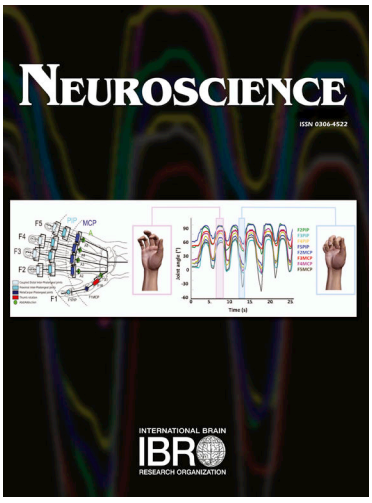

Research Article

Development of action potential waveform in hippocampal CA1 pyramidal neurons

Alberto Sánchez-Aguilera, Gonzalo Monedero, Asunción Colino, María Ángeles Vicente-Torres

PII: S0306-4522(20)30423-1
DOI: https://doi.org/10.1016/j.neuroscience.2020.06.042
Reference: NSC 19758

To appear in: *Neuroscience*

Received Date: 4 March 2020
Revised Date: 11 June 2020
Accepted Date: 29 June 2020

Please cite this article as: A. Sánchez-Aguilera, G. Monedero, A. Colino, M. Ángeles Vicente-Torres, Development of action potential waveform in hippocampal CA1 pyramidal neurons, *Neuroscience* (2020), doi: https://doi.org/10.1016/j.neuroscience.2020.06.042

Development of action potential waveform in hippocampal CA1 pyramidal neurons.

Alberto Sánchez-Aguilera1,2*, Gonzalo Monedero1, Asunción Colino1, María Ángeles Vicente-Torres 1*

1. Departamento de Fisiología, Facultad de Medicina, Universidad Complutense de Madrid (UCM); IdISSC. Avda Complutense s/n, 28040, Madrid, Spain.
2. Instituto Cajal, CSIC. Avda Doctor Arce 37, 28002, Madrid, Spain.

Running title: Development of action potential

*Authors for correspondence and proofs:

Alberto Sánchez-Aguilera
Instituto Cajal. CSIC
Avda. Doctor Arce 37. 28002, Madrid. Spain
Phone: 34-1-91 585 43 59
e-mail: asalopez@cajal.csic.es

María Ángeles Vicente-Torres
Departamento de Fisiología. Facultad de Medicina. Universidad Complutense de Madrid
Avda. Complutense s/n. 28040 Madrid. Spain
Phone: 34-1-91 394 1431
e-mail: mavictor@med.ucm.es

Section editor: Dr. J.N. Sanes

ABBREVIATIONS

4-AP	4-aminopiridine
ACSF	Artificial cerebrospinal fluid
AP	Action potential
CNQX	6-cyano-7-nitro-quinoxaline-2,3-dione
EGTA	Ethylene glycol-bis(β-aminoethyl ether)-N,N,N′,N′-tetraacetic acid
HEPES	4-(2-hydroxyethyl)-1-piperazineethanesulfonic acid
I_A	A-type potassium current
I_{Na}	Sodium current
P9-19	From 9 to 19 postnatal days
PBS	0.01 M phosphate-buffered saline pH 7.4
PBS-T	PBS containing 0.1 % of Tween 20
PTX	Picrotoxin
W2 / W3	Second / third postnatal week

ABSTRACT

CA1 pyramidal neurons undergo intense morphological and electrophysiological changes from the second to third postnatal weeks in rats throughout a critical period associated with the emergence of exploratory behaviour. Using whole cell current-clamp recordings in vitro and neurochemical methods, we studied the development of the somatic action potential (AP) waveform and some of the underlying channels in this critical period. At the third postnatal week, APs showed a more hyperpolarized threshold, higher duration and amplitude. Subthreshold depolarization broadened APs and depolarized their peak overshoots more pronouncedly in immature neurons (2 weeks old). These features were mimicked by pharmacologically blocking the fast-inactivating A-type potassium current and matched well with the higher concentrations of $K_v4.2$ and $K_v4.3$ and the lower concentrations of BK and $K_v1.2$ channels detected by Western blotting. Repetitive stimulation with high frequency trains (50 Hz) reproduced AP broadening associated to inactivation of the A-type current in immature cells. Moreover, repetitive firing showed changes in AP amplitude consistent with the inactivation of both sodium and potassium subthreshold currents, which resulted in higher AP amplitudes in the more immature neurons. We propose that maturation of AP waveform and excitability in this critical developmental period could be related to the onset of exploratory behaviours.

KEYWORDS: Development; CA1 pyramidal neurons; action potential; neuronal excitability; potassium channels; sodium channels.

HIGHLIGHTS

Action potentials in CA1 pyramidal neurons changed from 2 to 3 postnatal weeks.

Partial removal of I_A strongly modified the action potential in less mature cells.

Expression of Nav1.6, BK and Kv1.2 channels increased from 2 to 3 postnatal weeks.

Expression of Nav1.2, Kv4.2 and Kv4.3 channels decreased from 2 to 3 postnatal weeks.

Excitability due to active properties increased in these cells from week 2 to week 3.

INTRODUCTION

The first weeks of development are a critical period for the functional maturation of the hippocampus in rodents. Throughout this time, hippocampal neurons undergo intense morphological changes, including neuronal growth and ramification of axonal and dendritic branches (Pokorny and Yamamoto, 1981a, 1981b), with establishment of synaptic connections (Hsia et al., 1998). They also exhibit maturation of their passive electrophysiological properties. For instance, the resting potential of CA1 pyramidal neurons hyperpolarized and their membrane resistance and time constant decreased after maturation (Spigelman et al., 1992; Isagai et al., 1999; Giglio and Storm, 2014).

Active properties also mature during this period. Several studies have described some changes in action potential (AP) waveform, in particular a reduction of its duration and an increase in its amplitude (Spigelman et al., 1992; Isagai et al., 1999; Sánchez-Alonso et al., 2010). These changes are accompanied by changes in the transient sodium current (Costa, 1996) and in several potassium currents (A-type, D-type, BK and delayed rectifier) (Spigelman et al., 1992; Costa et al., 1994; Klee et al., 1995; Giglio and Storm, 2014). Moreover, the firing pattern of CA1 pyramidal neurons evolved from regular-spiking in the first postnatal days to burst-spiking during the second-third weeks, and returned to regular-spiking in mature neurons, a developmental process dependent on voltage-activated calcium currents (Costa et al., 1991; Chen et al., 2005; Metz et al., 2005; Sánchez-Alonso et al., 2010; Sánchez-Aguilera et al., 2017).

Previous studies from our group have analysed developmental changes of somatic AP from CA1 pyramidal neurons of developing hypothyroid animals, spanning up to postnatal weeks (Sánchez-Alonso et al., 2010, 2012), when eyes open and exploratory behaviour begins (Langston et al., 2010; Wills et al., 2010). The aim of the current research was to study in-depth the physiological changes in the developing AP waveform from the second postnatal week (W2; between 9 and 12 postnatal days; P9-12) to the third week (W3; between 16 and 19 postnatal days; P16-19). For that purpose, the AP waveform was firstly studied using an experimental approach in which all the currents involved in AP generation were initially available, and secondly after their partial inactivation by subthreshold depolarization. The molecular basis of the developmental changes detected in the currents underlying AP generation was then evaluated by pharmacological treatment and by quantifying the expression of some ion channels in the CA1 area. Finally, we analysed the developing AP waveform throughout repetitive firing.

EXPERIMENTAL PROCEDURES

Ethical approval

All experimental procedures were performed according to the European Union guidelines (2003/65/CE) and Spanish legislation (R.D. 1201/2005 and L.32/2007) for animal research and were approved by the Ethics Committee of Universidad Complutense de Madrid.

Slice preparation

Wistar rats from P9-12 (N= 26 animals) or P16-19 (N=21 animals) groups of age were used to prepare hippocampal slices (400 μm). Animals were decapitated, and the hippocampi quickly dissected in cold 95 % O_2 / 5 % CO_2 artificial cerebrospinal fluid (ACSF). Transverse hippocampal slices, taken from the middle portion of the dorsoventral axis, were cut and stored in a holding chamber at room temperature (27 - 29 ºC) for at least 1 h in 95 % O_2 / 5 % CO_2 ACSF. The composition of the ACSF was (in mM): 120 NaCl, 2.5 KCl, 2.5 $CaCl_2$, 1.3 $MgCl_2$, 26.2 $NaHCO_3$, 11 glucose, pH 7.3-7.4 when balanced with 95 % O_2 / 5 % CO_2.

Recordings in hippocampal slices

The slices were individually transferred to a submerged recording chamber. A peristaltic pump (Gilson) was used to perfuse 95 % O_2 / 5 % CO_2 ACSF to the recording chamber with a constant flow rate of 1.5 - 2 mL / min.

"Blind" whole-cell patch-clamp recordings in current-clamp mode were made from CA1 pyramidal neurons. Pyramidal neurons were identified by their position inside the *stratum pyramidale* and their electrophysiological properties. *Post-hoc* segregation between superficial and deep pyramidal neurons was not performed in this study. These experiments were performed with patch pipettes (pulled from borosilicate glass capillaries. Harvard Apparatus) filled with (in mM): 125 K gluconate, 8 NaCl, 10 HEPES, 3 Tris-ATP, 0.3 GTP, 2 $MgCl_2$, 20 phosphocreatine, 0.5 $CaCl_2$, 10 EGTA, and 50 U / mL creatine phosphokinase (pH 7.3 adjusted with KOH, osmolarity ~300 mOsm). Patch pipettes filled with this solution had resistances of ~5 - 10 MΩ. 6-cyano-7-nitro-quinoxaline-2,3-dione (CNQX; 10 μM) and picrotoxin (PTX; 100 μM) were included in the ACSF to block fast excitatory and inhibitory postsynaptic potentials respectively.

Current-clamp recordings were acquired with an Axoclamp 2A amplifier and a Digidata 1322 (Molecular Devices). Series resistance and membrane capacitance were compensated. Recordings

were performed at room temperature (27 – 29 ºC). Pyramidal neurons with a stable resting potential of at least −60 mV and with AP overshoots depolarized more than 0 mV were included in this study. Neurons with series resistance higher than 60 MΩ were discarded. Input resistance at –80 mV was calculated from the steady-state voltage measured in response to a 300 ms square pulse with a current intensity of –20 pA.

Electrophysiological data analysis

Parameters of the APs generated by depolarizing pulses (5 ms, 1 s square or 1 s depolarizing ramp) were analysed with Clampfit 10.2 (Molecular Devices). The AP threshold was defined as the first membrane potential with dV/dt higher than 15 mV / ms. The AP peak overshoot was the most depolarized value of the AP. The amplitude was measured as the difference between the peak voltage and AP threshold. The AP half-width was the spike duration at half its amplitude. The depolarization rate was measured as the mean rate between 10 % and 90 % of the AP amplitude. The repolarization rate was measured as the mean rate between 0.3 ms after the peak and 50 % of the AP amplitude.

For the repetitive firing study, APs were elicited by a train of ten 5 ms-pulses, at 10 Hz and 50 Hz, with enough intensity to generate an AP in each pulse. CA1 pyramidal neurons from P16-19 usually have a burst-spiking firing pattern mediated by the low-voltage-activated calcium current and sensitive to low concentrations of nickel (Sánchez-Alonso et al., 2010; Sánchez-Aguilera et al., 2017). Therefore, in these experiments 100 µM of nickel was applied to the bath to avoid generating 2-3 APs in the first pulse of the train.

Current-clamp recordings were performed from a holding membrane potential of approximately –80 mV by controlling the injection of negative continuous current by the amplifier. Recordings and membrane potentials were corrected for their junction potential.

Plots were made with Origin 6.0 and customized scripts with MATLAB (Mathwork v.2019a).

Protein extraction

The CA1 area of both hippocampi (N= 20 animals) was dissected in cold 95 % O_2 / 5 % CO_2 ACSF and stored at –80 °C until protein extraction was carried out. Four CA1 areas from two rats were pooled per sample and homogenized in cold lysis buffer: 0.01 M phosphate-buffered saline (1.47 mM KH_2PO_4, 8.10 mM Na_2HPO_4, 2.67 mM KCl, 137.93 mM NaCl), pH 7.4 (PBS), containing 5

mM EGTA, 5 mM dithiothreitol, 10 mM sodium fluoride, 1 mM phenylmethanesulfonyl fluoride, 1mM sodium orthovanadate and 2X (1 tablet / 5 ml) of a protease inhibitor cocktail (Roche, Basel, Switzerland). Homogenates were centrifuged at 3000 x g at 4 °C for 10 min to remove the nuclei and the resulting supernatant was further centrifuged at 150000 x g for 17 min at 4 °C. The pellet (membrane fraction) was then resuspended in cold lysis buffer and stored at –80 °C until analysed. Protein concentrations were determined by using the Bio-Rad Protein Assay dye reagent (Bio-Rad, Hercules, CA, USA) with bovine serum albumin as a protein standard.

Western blot analysis

Equal amounts (10 - 35 µg) of total protein were loaded per lane on 6.5 or 8 % gels and separated by SDS-PAGE. After separation, proteins were transferred onto nitrocellulose membranes (Amersham Biosciences, Piscataway, NJ, USA). The membranes were stained with Ponceau S and then blocked with 5 % non-fat milk in PBS containing 0.1 % of Tween 20 (PBS-T) and incubated with mouse anti-$Na_v1.2$ 1:600 (Acris Antibodies, San Diego, CA, USA), rabbit anti-$Na_v1.6$ 1:600 (GeneTex, Irvine, CA, USA), mouse anti-$K_v1.2$ 1:20000 (NeuroMab, Davis, CA, USA), rabbit anti-BK 1:600 (Acris Antibodies, San Diego, CA, USA), rabbit anti-$K_v4.2$ 1:4000 or rabbit anti-$K_v4.3$ 1:2000 (Alomone Laboratories, Jerusalem, Israel). Immunodetection was done using peroxidase-conjugated secondary antibodies and enhanced chemiluminescence with ECL reagents (Amersham Biosciences, Piscataway, NJ, USA). Semi-quantitative analysis of the bands was performed using laser-scanned densitometric analysis (Quantity One, Bio-Rad Hercules, CA, USA) and the individual ratios to β-actin densities were normalized with respect to the more immature age (2 weeks).

Statistical analysis

Statistical analysis was performed with SPSS 17.0. Normality was evaluated with a Kolmogorov-Smirnov test and equal variances were tested with a Levene test. For consistency in the analysis strategy, we chose the same test for similar analyses. Comparisons between two independent samples were analysed using a non-parametric Mann-Whitney U test. Comparisons between two states in the same cell were analysed with a non-parametric Wilcoxon signed-rank test. Comparison of the action potential properties during repetitive firing and input-output curves between P9-12 and P16-19 were analysed using a two-way ANOVA. $P < 0.05$ was considered as statistically significant. Data are

presented as median and interquartile range in figures. In text, data are presented as median (percentile 25, percentile 75).

Chemicals

All the chemicals and drugs were from Sigma-Aldrich (St. Louis, MO, USA), except where noted otherwise.

RESULTS

Development of the somatic action potential in CA1 pyramidal neurons

Previous studies have shown that AP duration decreased whereas AP amplitude progressively increased throughout the first postnatal weeks when stimulation was carried out from the resting potential or with long depolarizing pulses (Spigelman et al., 1992; Isagai et al., 1999; Sánchez-Alonso et al., 2010). Here, we first analysed in W2 (N=68 cells) and W3 (N=55 cells) groups the somatic AP waveform of CA1 pyramidal neurons in conditions in which all the currents involved were totally available. To reduce partial current inactivation, APs were elicited by the application of a short (5 ms) threshold depolarizing current pulse at –80 mV (Fig. 1A).

In these conditions, AP duration increased approximately 29 % with age from W2 to W3 neurons ($U_{68,55}$= 172.5, P<0.0001. Fig. 1B, D). This increment in half–width was associated with a decrease in the repolarization rate from W2 to W3 ($U_{68,55}$= 687.0, P < 0.0001, Mann-Whitney U test. Fig. 1B – D). Furthermore, AP amplitude increased approximately 25 % from W2 to W3 ($U_{68,55}$= 104.0, P<0.0001, Mann-Whitney U test. Fig. 1B, D) because of the AP threshold hyperpolarization and the depolarization of the peak overshoot (Threshold: $U_{68,55}$= 399.5; Peak: $U_{68,55}$= 280.0, P < 0.0001 for both parameters, Mann-Whitney U test. Fig. 1B – D). Finally, the depolarization rate was significantly faster in W3 neurons ($U_{68,55}$= 113.5, P < 0.0001, Mann-Whitney U test. Fig. 1B, D). Taken together, the increase in AP duration and amplitude from W2 to W3 neurons suggested a change in the ratio between depolarizing and repolarizing currents or in the ratio between sodium and potassium currents in general.

Effect of subthreshold depolarization on developing somatic action potential

In hippocampal pyramidal neurons at least three types of potassium currents have major roles in the AP repolarization: A-type and D-type voltage-dependent and BK calcium-activated potassium currents (Storm, 1990; Bean, 2007). A-type and D-type potassium currents are fast activated at subthreshold potentials, where I_A inactivates rapidly and I_D inactivates more slowly (Storm, 1988, 1990; Bean, 2007; Johnston et al., 2010). Furthermore, a substantial component of transient sodium current is activated at subthreshold potentials in CA1 neurons (Carter et al., 2012). To better understand the consequences of partially inactivating the subthreshold activated currents involved in the generation of somatic AP in W2 and W3 neurons, we applied threshold depolarizing pulses of 5 ms and 1 s duration from a membrane potential of -80 mV (Fig. 2, N_{W2}= 25 cells, N_{W3}= 18 cells). When the neuron fired more than one AP (as in the example of Fig. 2A), only the first AP generated was studied.

In comparison to the 5 ms pulse, the longer and weaker (1 s) threshold pulse elicited APs with higher duration accompanied by a slower repolarization rate (Fig. 2B - D). These changes were much more prominent in the more immature neurons. Interestingly, the APs generated by the longer pulse in the more immature neurons also showed increased amplitude and a more depolarized overshoot (Fig. 2B, E, F). However, there was only mild depolarization of the AP threshold in the APs generated by the longer pulse (P9-12: 5 ms: -54.40 (-56.17, -52.11) mV; 1 s: -53.33 (-54.53, -51.18) mV, Z= -2.476, P = 0.0133, Wilcoxon signed-rank test; P16-19: 5 ms: -59.58 (-61.39, -54.82) mV; 1 s: -56.64 (-59.21, -53.13) mV, Z= -3.507, P = 0.0005, Wilcoxon signed-rank test), and a non-statistically significant trend in the reduction of the depolarization rate (P9-12: 5 ms: 140.63 (131.36, 160.71) mV/ms; 1 s: 137.42 (124.08, 153.25) mV/ ms, Z= -1.843, P = 0.0653, Wilcoxon signed-rank test; P16-19: 5 ms: 209.09 (197.42, 226.35) mV/ms; 1 s: 204.41 (196.11, 221.86) mV/ ms, Z= -2.461, P = 0.0139, Wilcoxon signed-rank test).

Long (1s) square pulses allowed only a small window of opportunity for firing APs at the beginning of the pulse (Fig. 2G), which could be associated to the hyperpolarization of the membrane due to activation of the M-current. In a subthreshold pulse, the shorter membrane time constant of W3 neurons (Sánchez-Alonso et al., 2012) allowed them to reach their most depolarized voltage faster than W2 neurons (Fig. 2G). Consequently, the onset for AP firing was longer in the more immature neurons (Fig. 2H), which could contribute to increasing the inactivation percentage of low threshold currents and consequently AP duration and amplitude.

To prevent AP latency differences between ages, which could affect AP parameters, APs elicited by brief (5 ms) threshold pulses were compared with those elicited by rising current pulses consisting of

1-second-depolarizing ramps with low intensity, just enough to generate an AP at the end of the ramp (Fig. 3, N_{W2}= 17 cells, N_{W3}= 14 cells). When the neuron fired several APs (as in the example of Fig. 3A), the first AP generated was studied.

The AP duration was significantly higher and the repolarization rate slower when the AP was elicited by the 1s-ramp in comparison to the 5 ms stronger pulse at both age periods (Fig. 3B - D). However, neurons from W2 group experienced a significantly more dramatic broadening than W3 neurons (Fig. 3B - D).

Furthermore, AP amplitude in W2 neurons was higher when the AP was generated by a 1 s current ramp than by a 5 ms stronger pulse stimulation (Fig. 3B, E). That higher AP amplitude in response to a current ramp was accompanied by a peak overshoot, which was approximately 97 % more depolarized (Fig. 3B, F). In contrast to W2 neurons, AP amplitude in W3 neurons was not significantly different when using both stimulation protocols (Fig. 3B, E).

Notably, subthreshold depolarization by the ramp only significantly depolarized the AP threshold in neurons from W3 (P9-12: 5 ms: -56.20 (-59.18, -54.70) mV; Ramp: -56.71 (-57.63, -53.43) mV, Z= 0.923, P = 0.3560, Wilcoxon signed-rank test; P16-19: 5 ms: -63.09 (-64.49, -60.96) mV; Ramp: -61.25 (-62.44, -60.25) mV, Z= -3.296, P = 0.0001, Wilcoxon signed-rank test). These results could suggest that neurons from W2 undergo a similar subthreshold inactivation of both sodium and potassium currents, while neurons from W3 experience major inactivation of the transient sodium current. The subthreshold depolarization by the ramp did not change the depolarization rate (P9-12: 5 ms: 145.09 (123.51, 164.94) mV/ ms; Ramp: 142.64 (124.37, 160.99) mV/ ms, Z= -2.485, P = 0.0129, Wilcoxon signed-rank test; P16-19: 5 ms: 203.33 (185.02, 217.03) mV/ ms; Ramp: 194.73 (183.68, 208.11) mV/ ms, Z= -1.538, P = 0.1240, Wilcoxon signed-rank test).

In summary, a sustained subthreshold depolarization more strongly increased AP duration and amplitude in W2 neurons (Figs. 2, 3). These results are in agreement with a higher inactivation of repolarizing low threshold activated potassium currents in W2 neurons, which could be a consequence of a different current expression throughout development.

Effect of 4-aminopiridine (4-AP) treatment on somatic action potential development

In order to more directly test the influence of low threshold potassium currents on developing AP waveform, we pharmacologically blocked them using 4-AP at two different concentrations: low concentration (30 μM) to block only slow-inactivating D-type potassium current and high

concentration (3 mM) to block both D-type and the A-type potassium currents (Mitterdorfer and Bean, 2002)**.** At a holding potential of –80 mV, APs were elicited with depolarizing 5 ms threshold current pulses in different sets of neurons treated with 4-AP 30 µM or 3 mM (Fig. 4).

Treatment with 30 µM 4-AP (N_{W2}= 12 cells, N_{W3}= 9 cells) similarly affected AP waveform in both age groups. In W2 and W3, it induced a slight and similar broadening (Fig 4B right) of the APs, which was accompanied by a small decrease in their repolarization rate (Fig 4C right), which was consistent with previous studies (Kole et al., 2007; Shu et al., 2007). Moreover, neither AP amplitude nor AP overshoot was significantly modified by treatment with 30 µM 4-AP at any age group (Fig. 4A, D, E).

In contrast, application of a high concentration (3 mM) of 4-AP differentially affected the somatic AP waveform in W2 (N=12 cells) and W3 neurons (N= 9 cells). Firstly, the more immature neurons dramatically showed more broadened APs after 3 mM 4-AP application (Fig 4F, Fig 4G-H right). Secondly, treatment with 3 mM 4-AP significantly increased AP amplitude and peak overshoot much more in neurons from W2 than in neurons from W3 (Fig 4F, 4I right and 4J right).

Thus, pharmacological experiments suggest a relevant role of the A-type current in modulating AP amplitude and duration at these developmental stages, mainly in the W2 period.

Development of the expression of ion channels involved in CA1 action potentials

To elucidate the molecular mechanisms underlying AP development in CA1 pyramidal neurons, we next analysed the expression of several sodium and potassium channels whose currents contribute to the AP waveform (N= 3 independent experiments for each ion channel). In CA1 pyramidal neurons, two sodium channel isoforms ($Na_v1.2$ and $Na_v1.6$) were identified by immunofluorescence (Lorincz and Nusser, 2008, 2010; Debanne et al., 2011). Furthermore, several potassium channel isoforms responsible for the D-type current ($K_v1.2$), A-type current ($K_v4.2$ and $K_v4.3$) and BK current were identified by PCR-RT and/or histoblotting (Martina et al., 1998; MacDonald et al., 2006; Alfaro-Ruíz et al., 2019). The expression of these ion channels in the hippocampal CA1 area of W2 (P9-10) and W3 (P18-19) rats was evaluated by Western blot (Fig. 5). Although the Western blot analysis focused on the channel isoforms present in pyramidal neurons, the contribution of other cell types could not be excluded, since the CA1 samples included other cell types present in the region. Specific antibodies were used to detect the expression of the pore forming subunits of the five voltage gated ion channels: $Na_v1.2$, $Na_v1.6$, $K_v1.2$, $K_v4.2$ and $K_v4.3$. In addition, total expression of

BK channels was analysed with an antibody that recognized a C-terminus region in the protein that remained constant among different isoforms, as described by the manufacturer (AP20653PU-N, Acris Antibodies).

We found that $Na_v1.2$ expression decreased in 3 independent experiments to 57.28 %, 41.69 % and 7.8 % in W3, considering W2 as 100 % ($U_{3,3}$= 0.0, P=0.0369, Mann-Whitney U test), while $Na_v1.6$ increased to 402.95%, 387.38 % and 246.13 % in W3, considering W2 as 100 % ($U_{3,3}$= 0.0, P=0.0369, Mann-Whitney U test) (Fig. 5A, B). With respect to the potassium channels, expression of both $K_v1.2$ and BK channels increased from W2 to W3 periods in 3 out of 3 independent experiments to: 256.48%, 501.56 % and 161.92 % for $K_v1.2$ in W3, considering W2 as 100 % ($U_{3,3}$= 0.0, P=0.0369, Mann-Whitney U test), and 517.17 %, 282.45 %, 238.35 % for BK in W3, considering W2 as 100 % ($U_{3,3}$= 0.0, P=0.0369, Mann-Whitney U test) (Fig. 5C, D). However, the expression of K_v4 channels responsible for the A-type current decreased with development in all 3 independent experiments to: 67.65%, 42.51 %, 37.09 % for $K_v4.2$ in W3, considering W2 as 100 % ($U_{3,3}$= 0.0, P=0.0369, Mann-Whitney U test), and 53.09%, 50.40 % and 62.76 % for $K_v4.3$ in W3, considering W2 as 100 % ($U_{3,3}$= 0.0, P=0.0369, Mann-Whitney U test) (Fig. 5E, F). These results are consistent with changes in the AP from W2 to W3: hyperpolarization of the AP threshold, increment of the AP amplitude and duration and less modulation by the low-voltage-activated A-type potassium current, which is both fast-activating and fast-inactivating.

Effect of repetitive firing on the waveform of developing action potential

In CA1 pyramidal neurons, inactivation of A-type and BK potassium currents has been involved in AP broadening during repetitive firing (Shao et al., 1999; Kim et al., 2005; Bean, 2007). During the period between W2 and W3 there is a reduction in the sensitivity of somatic AP to a high concentration of 4-AP (Fig. 4), accompanied by a change in relative expression of K_v4 and BK channels (Fig. 5). Therefore, we next studied the AP waveform of developing CA1 pyramidal neurons throughout repetitive firing. To control the timing for AP generation, we applied trains of ten 5-ms-current pulses at low (10 Hz) and high (50 Hz) frequencies, with enough intensity to elicit an AP in each pulse N_{W2}= 16 cells, N_{W3}= 11 cells.

We found consistent broadening from AP 1 to AP 10. At 10 Hz, the magnitude of the broadening was very small and similar in W2 and W3 (Half-width: P=0.7214 for age factor; Rep. rate: P= 0.8064 for age factor. 2-way ANOVA. Fig. 6B - D). However, AP duration increased, and repolarization rate decreased

much more in the more immature neurons at 50 Hz (Half-width: P<0.0001 for age factor; Rep. rate: P< 0.0001 for age factor. 2-way ANOVA Fig. 6B - D).

Interestingly, regarding AP amplitude and overshoot, two opposite behaviours were identified. At 10 Hz, AP amplitude decreased and AP overshoot became less depolarized from AP 1 to AP 10, where the magnitude of these changes was bigger in the more immature neurons (Amplitude: P < 0.0001 for age factor, 2-way ANOVA; Overshoot: P < 0.0001 for age factor, 2-way ANOVA. Fig. 6B, E, F). Meanwhile, at 50 Hz, APs from W2 neurons experienced a lower reduction of their amplitude and overshoot from AP 1 to AP 10. (Amplitude: P < 0.0001 for age factor, 2-way ANOVA; Overshoot: P < 0.0001 for age factor, 2-way ANOVA. Fig. 6B, E, F). Even, in W2 neurons, the APs following the first AP increased their amplitude and depolarized their overshoot with respect to AP 1. The different cumulative inactivation of the transient sodium current and A-type potassium current could explain this phenomenon, since an imbalance was observed between the depolarization and repolarization kinetics in W2 neurons. At 10 Hz, W2 neurons showed a slowdown of their AP depolarization rate throughout the train that was slightly greater than in W3 neurons (P < 0.0001 for age factor, 2-way ANOVA), and also slightly greater than the reduction in their repolarization rate (Depol. Rate reduction in W2 at AP 10: -17.89 (-24.19, -15.55) %; Repol. Rate reduction in W2 at AP 10: -14.34 (-18.14, -8.27) %, $U_{16,16}$= 61.0, P = 0.012, Mann-Whitney U test P = 0.012, Mann-Whitney U test). However, at 50 Hz, the slowdown of the AP depolarization rate in W2 was similar to that in W3 neurons (P=0.0677 for age factor, 2-way ANOVA) and it was much smaller than the reduction in its repolarization rate (Depol. Rate reduction in W2 at AP 10: -32.69 (-35.36, -23.90) %; Repol. Rate reduction in W2 at AP 10: -53.15 (-68.61, -46.10) %, $U_{16,16}$= 9.0, P < 0.0001, Mann-Whitney U test).

Development of intrinsic excitability in CA1 pyramidal neurons

In the previous condition, the neuron was forced to fire at fixed timestamps. To remove the timing control for AP firing and evaluate the intrinsic excitability of developing CA1 pyramidal neurons, we applied a series of 1 s suprathreshold somatic injection current steps at -80 mV with increasing intensity (Fig. 7A-B, N_{W2}= 26 cells, N_{W3}= 18 cells). Under these stimulation conditions, there was a bimodal behaviour in the input-output curve depending on the current intensity injected (P < 0.0001 for the age factor; P < 0.0001 for the interaction between current intensity and age factors, 2-way ANOVA. Fig. 7B). With current injections under 300 pA, the firing frequency was higher in P9-12 neurons compared to P16-19 neurons, probably due to the higher input resistance in the more immature neurons (P9-12: 186.89 (160.76, 227.28) MΩ; P16-19: 94.44 (87.41, 104.69) MΩ, $U_{26,18}$= 3.0, P < 0.0001, Mann-

Whitney U test) as others have also reported (Spigelman et al., 1992; Sánchez-Alonso et al., 2012; Giglio and Storm, 2014). Indeed, the rheobase was lower in P9-12 neurons (P9-12: 130.00 (100.00, 132.50) pA; P16-19: 200.00 (180.00, 220.00) pA, $U_{26,18}$= 15.5, P < 0.0001, Mann-Whitney U test), despite the fact that the AP threshold was more depolarized (P9-12: -54.85 (-56.09, -52.13) mV; P16-19: -59.18 (-60.75, -56.23) mV, $U_{26,18}$= 15.5, P < 0.0001, Mann-Whitney U test). However, with current injections over 450 pA W3 neurons fired more APs than W2 neurons (Fig. 7B). Neurons from W2 required much less current to reach their maximum firing frequency (P9-12: 350.00 (300.00, 380.00) pA; P16-19: 550.00 (505.00, 622.50) pA, $U_{26,18}$= 2.5, P < 0.0001, Mann-Whitney U test). To remove the effect of the neuron passive properties on CA1 pyramidal neurons' firing frequency, a second input-output curve was built by standardization of the input to the theoretical membrane potential that the membrane would have reached according to the Ohm's law ($\Delta V_m = I_{injected} * R_m$). In this corrected second curve (N_{W2}= 26 cells, N_{W3}= 18 cells), W2 neurons showed a lower firing frequency than W3 neurons for the same theoretical membrane potentials (P < 0.0001 for the age factor, 2-way ANOVA. Fig. 7C, D). Furthermore, neurons from W2 had a lower maximum firing frequency (Fig. 7D - F).

DISCUSSION

We evaluate developmental kinetics of the AP waveform in CA1 pyramidal neurons at a period around eye opening and the onset of exploratory behaviour: increasing AP duration and amplitude from W2 (P9-12) to W3 (P17-19) age. We show how partial inactivation of low-voltage activated potassium currents was involved in AP generation by subthreshold depolarization or by pharmacological blockage with high concentration of 4-AP: AP duration and amplitude increased more pronouncedly in W2 neurons. Furthermore, there were associated changes in the expression of several sodium and potassium channels from W2 to W3. Finally, neuronal excitability and the changes in the AP waveform throughout repetitive firing were also different between two- and three-week-old neurons.

Development of somatic action potential waveform in naïve conditions

In this study, APs were recorded at a membrane potential (-80 mV) hyperpolarized enough to reduce partial inactivation of low-voltage-activated currents. In these conditions, maturation of the AP waveform from W2 to W3 was observed: the more immature neurons fired APs with lower duration and amplitude (Fig. 1). The increment in AP amplitude from W2 to W3 is in agreement with other

studies (Spigelman et al., 1992; Isagai et al., 1999; Sánchez-Alonso et al., 2010). However, those authors reported similar or reduced AP durations during the second and third weeks of postnatal development. A likely explanation for this discrepancy could be based on the voltage from which the spikes were evoked, since APs were elicited from resting potential and / or using protocols which depolarized the membrane for several tens of ms before inducing the AP. Keeping the membrane more depolarized could preferentially broaden the spikes from the more immature neurons, as is further discussed in the next epigraph.

The increase in AP duration and reduction of the repolarization rate from W2 to W3 age (Fig. 1) were associated to changes in the expression of potassium channels involved in AP repolarization: decrease in channels involved in I_A current (K_v4.2 and K_v4.3) and increase in channels involved in I_D (K_v1.2) and BK currents (Fig. 5). These results are consistent with previous reports showing a relevant role of A-type potassium current in AP repolarization of immature hippocampal CA1 neurons. As postnatal development progressed, other potassium currents with slower kinetics, such as D-type or BK currents, increased (Spigelman et al., 1992; Costa et al., 1994; Klee et al., 1995; Giglio and Storm, 2014). Furthermore, the prevalence of A-type current in the more immature neurons is supported by single-cell PCR-RT studies, which identified at P11-16 the mRNAs of K_v4.2 and K_v4.3 in 86 % of CA1 pyramidal cells analysed, while just 34 % of them expressed the mRNA of K_v1.2 (Martina et al., 1998). Likewise, total mRNA of BK channels increased from P7 to P35 in the hippocampus (MacDonald et al., 2006). In contrast, a recent histoblot study in mice has reported a peak of expression at P15 for K_v4.2 in CA1 area and at P30 for K_v4.3 in CA3 (Alfaro-Ruíz et al., 2019). This discrepancy could be due to differences in the samples between that study and ours. While histoblot quantifications were carried out on the stratum radiatum of four horizontal brain sections per age (Alfaro-Ruíz et al., 2019), the Western blot samples of the current study were pools of four CA1 areas (CA1s of both hippocampi from two animals) per age. Therefore, both quantifications differed in the proportion of pyramidal cells versus interneurons and the hippocampal area and layer considered, which are factors related to differences in K_v4.2 and K_v4.3 expressions (Martina et al., 1998; Alfaro-Ruíz et al., 2019). Furthermore, this discrepancy could suggest differences in K_v4.2 and K_v4.3 along the dorsal-to-ventral axis of the hippocampus and between CA1 and CA3, which would be worthy of further exploration.

The increase in AP amplitude throughout development was a consequence of several factors, including hyperpolarization of the AP threshold, depolarization of the AP overshoot and a faster depolarization rate (Fig. 1). These data fit well with the increment in the transient sodium current and the leftward shift of its activation curve described throughout development (Costa, 1996). In

addition, expression of sodium channels in the CA1 area evolved from $Na_v1.2$ to $Na_v1.6$ isoforms at this developmental period (Fig. 5). This gradual replacement of $Na_v1.2$ by $Na_v1.6$ during development was also reported in the axon initial segment of retinal ganglion cells (Boiko et al., 2003) in parallel with the emergence of repetitive firing and the speeding-up of the recovery from inactivation of the sodium current (Wang et al., 1997). Furthermore, $Na_v1.6$ channels display more hyperpolarized activation than $Na_v1.2$ channels (Rush et al., 2005). In CA1 pyramidal neurons, an important role of $Na_v1.6$ channels has been described in AP initiation, since they activate at more negative voltages than other Na_v isoforms (Royeck et al., 2008; Hu et al., 2009). However, the A-type potassium current may also contribute to regulating AP amplitude, since a subthreshold role in depolarizing the AP threshold has been described (Kim et al., 2005). A previous study from our lab has shown in CA1 pyramidal neurons that high I_A in developing hypothyroid rats contributed to depolarizing their AP threshold and to increasing their intrinsic excitability (Sánchez-Alonso et al., 2012). Moreover, our data (Fig 2-4, 6) suggest that in naïve conditions, the A-type potassium current has a suprathreshold role in controlling AP overshooting. In more immature neurons, with lower $Na_v1.6$ channel expression and slower depolarization, the dominance of A-type potassium current would depolarize the AP threshold and counteract the sodium inward current, producing a brake in the depolarization, which in turn would reduce the theoretical overshooting. In more mature neurons the faster depolarization rate and the reduction in $K_v4.2$ and $K_v4.3$ channels dismiss the contribution of I_A in controlling the AP threshold and overshooting. Therefore, the reduction of the A-type type potassium current may also contribute to increasing the AP amplitude during development. We want to highlight that temperature increases peak current and accelerates activation and inactivation kinetics of currents such as sodium and A-type and D-type potassium currents (Russell et al., 1994; Rosen, 2001; Sarria et al., 2012). In consequence, AP amplitude and duration are reduced with high temperature (Money et al., 2005). The relatively low temperature in our recordings (27-29°C) could increase AP amplitude and width. The magnitude of the involved currents would be smaller at low temperature, but slowing their kinetics could have allowed us to better trace the changes in the AP waveform between W2 and W3.

Development of action potential waveform after partial inactivation of some of the currents involved

Inactivation of some of the low threshold currents involved in AP generation by subthreshold depolarization mostly affected the AP waveform in the more immature group (P9-P12) (Figs. 2, 3). Slow depolarization increased AP duration and amplitude more in W2 neurons (Figs. 2, 3), as did the

application of 3 mM 4-AP, but not 30 μM (Fig. 4), which supports a predominant inactivation of the A-type current in W2 neurons as a consequence of their higher expression of $K_v4.2$ and $K_v4,3$ channels (Fig. 5). The contribution of low threshold A-type potassium current to somatic AP duration and amplitude decreased in more mature neurons. Nevertheless, a slight effect remained in P16-19 neurons, as the application of 3 mM 4-AP also increased AP duration and amplitude in these more mature neurons (Fig. 4).

Several currents contribute to AP repolarization in developing CA1 pyramidal neurons. Both channel expression (Fig. 5) and current isolation (Spigelman et al., 1992; Costa et al., 1994; Klee et al., 1995; Giglio and Storm, 2014) showed that the more immature neurons had low D-type and BK currents, which would not likely be able to compensate for the effect of A-type current inactivation on AP repolarization. Thus, their AP duration increased. Otherwise, the preferential increase in amplitude and overshoot of the AP generated after a subthreshold depolarization in the more immature neurons could correlate with the balance between depolarizing and repolarizing currents. The outward fast-activating potassium currents (A-type and D-type) represent a brake in AP depolarization, since voltage clamp recordings using a previously recorded AP as a command voltage showed that the activation of I_A and I_D overlapped with the final part of the AP depolarizing phase in CA3 pyramidal neurons (Mitterdorfer and Bean, 2002). Under I_A-inactivation associated to subthreshold depolarizing conditions, the I_A-brake of depolarization would be released, and AP amplitude would mostly increase in the more immature neurons, as observed in figures 2 and 3. Together with the partial inactivation of I_A, a fraction of the transient sodium current may also be inactivated by a slow, subthreshold depolarization (Carter et al., 2012). In our study, the subthreshold inactivation of the I_{Na} depolarized the AP threshold mainly in W3 neurons (Figs. 2, 3). This phenomenon could be explained by greater subthreshold inactivation of I_A in W2 cells compared to W3 cells, which would counteract depolarization of the AP threshold by I_{Na} inactivation.

Action potentials during repetitive firing in developing neurons

The AP changes its waveform during repetitive firing due to the activation and inactivation of voltage- and calcium-dependent channels (Ma and Koester, 1996; Shao et al., 1999; Kim et al., 2005; Bean, 2007; Gu et al., 2007). In the present study, there were frequency-dependent changes in AP waveform throughout the trains that affected AP duration and amplitude, which were the major changes observed with the higher stimulation frequency (50 Hz).

A progressive AP broadening from the 1st to the 10th AP of the 50 Hz train was observed, associated with a reduced repolarization rate, which was more marked in immature neurons (Fig. 6). Previous studies in adult CA1 pyramidal neurons related AP broadening throughout a long pulse (50 and 100 ms) to the cumulative inactivation of BK-type channels (Shao et al., 1999; Gu et al., 2007). Meanwhile, studies in CA1 pyramidal neurons in culture showed AP broadening in response to trains of brief pulses, which were related to the cumulative inactivation of the $K_v4.2$ channel, which inactivates rapidly but recovers from inactivation relatively slowly (Kim et al., 2005). I_A is a major repolarizing current in immature hippocampal CA1 pyramidal neurons (Spigelman et al., 1992; Kim et al., 2005; Sánchez-Alonso et al., 2012), and its channels, $K_v4.2$ and $K_v4.3$, were more abundant in W2 neurons (Fig. 5). Moreover, the A-type potassium current is particularly sensitive to experiencing cumulative inactivation during high-frequency firing (Ma and Koester, 1996; Kim et al., 2005; Gu et al., 2007). Taking all of the above into consideration, the extensive AP broadening in W2 neurons throughout repetitive firing at 50 Hz might be explained on the basis of the cumulative inactivation of the A-type potassium current. AP broadening at the 10th AP of the train (Fig. 6) was higher than the AP elicited by a 1 s threshold ramp (Fig. 3), which suggests higher inactivation of A-type current under repetitive firing. This could be due to the fact that only the component of the A-type current already active at subthreshold potentials is inactivated under the ramp stimulation protocol. Similarly slow subthreshold depolarization in immature CA3 pyramidal neurons inactivated just about half of the A-type potassium current (Mitterdorfer and Bean, 2002). In contrast, in W3 neurons, other potassium currents such as BK and D-type, whose channel expression increased with development (Fig. 5) could contribute to a more effective repolarization during high-frequency firing. Furthermore, the delayed-rectifier potassium current could help AP repolarization in W3 neurons, since it increased with development in CA1 pyramidal neurons (Spigelman et al., 1992; Costa et al., 1994; Klee et al., 1995), and K_v2 channels had a greater role in AP repolarization when other potassium channels were partially inactivated as during subthreshold depolarization or during episodes of high-frequency activity (Du et al., 2000; Bean, 2007; Liu and Bean, 2014).

Regarding AP amplitude during repetitive firing stimulation at 10 Hz, it progressively decreased in both age groups, where this reduction was more pronounced in W2 neurons. This could be related to the predominance at early stages of development of sodium currents with faster inactivation components (Costa, 1996) or to the slower recovery from inactivation associated with the $Na_v1.2$ isoform (Wang et al., 1997; Rush et al., 2005), whose expression is higher in W2 neurons (Fig. 5). At 50 Hz, AP amplitude also progressively decreased from the 1st to the 10th AP in W3 neurons (Fig. 6). In contrast, the amplitude of individual APs elicited after 1 s subthreshold depolarization in W3

neurons (Fig. 3) did not change in comparison with APs elicited by a short pulse (5 ms). These results suggest that the transient sodium current was partially and cumulatively inactivated during repetitive firing, since an important reduction in the sodium current is necessary in order to detect a significant decrease in the AP maximum depolarization rate or AP amplitude (Madeja, 2000). A-type potassium current could probably be inactivated but its contribution in W3 neurons was small. However, the AP amplitude profile changed in W2 neurons under 50 Hz train stimulation: it was reduced less in W2 neurons than in W3 neurons and it even increased from AP 1st to 4th (Fig. 6). These results pointed to an age-related change in the balance between depolarizing and repolarizing currents, probably because they experience unequal inactivation. While the depolarization rate was progressively reduced, the repolarization rate exhibited the highest reduction during the first APs of the train, which could be due to the very fast inactivation of the A-type current in comparison to the sodium current (Ma and Koester, 1996; Gu et al., 2007). These data suggest that in W2 neurons, inactivation of the hyperpolarizing A-type potassium current, whose channels are more abundant at this age (Fig. 5), could contribute to increasing AP overshoot and amplitude under high frequency stimulation.

Postnatal maturation of intrinsic excitability interacts with other developmental programs such as neuronal growth, ramification of axonal and dendritic branches and synapses formation (Moody, 1998). In the current study, neurons from W2 reached their maximum firing frequency with weaker stimuli than neurons from W3. This is probably because of the reduction in the input resistance from W2 to W3, also observed throughout development by other authors (Spigelman et al., 1992; Sánchez-Alonso et al., 2012; Giglio and Storm, 2014). However, the excitability versus similar depolarizing stimuli increased from W2 to W3, together with the maximum firing capability (Fig 7). On the one hand, the increase in the transient sodium current (Costa, 1996) and the decrease in the A-type current during development hyperpolarized the AP threshold (Fig. 1). On the other hand, the higher contribution of voltage- and calcium-dependent potassium currents (Spigelman et al., 1992; Costa et al., 1994; Klee et al., 1995; Giglio and Storm, 2014), facilitated a faster and more effective repolarization and a faster voltage-dependent recovery from inactivation of the sodium channels (Kuo and Bean, 1994) during repetitive firing. Normal maturation of these currents is crucial for the correct establishment of some intrinsic and synaptic forms of plasticity in which the AP waveform plays a major role. For example, coupling between T-type calcium current and A-type potassium current narrows the AP of CA1 pyramidal neurons against sustained subthreshold depolarizations from around P16 (Sánchez-Aguilera et al., 2014). Moreover, disruptions of the physiological AP waveform may impact the calcium influx in the presynaptic terminal and change the release

probability and pre-synaptic short-term plasticity (Colino et al., 1998; Shu et al., 2006). Therefore, maturation of these currents in CA1 pyramidal neurons allows a more efficient processing of their inputs in a stage which is critical for axonal and dendritic growth and for the establishment of synapses.

Functional significance

The hippocampus receives information from all sensory modalities and participates in episodic memory, including spatial memory (Eichenbaum, 2017). Hippocampal place cells participate in space coding and experience representation. They have a spatial receptive field, and their firing depends on self-motion and visual inputs (Tan et al., 2016; Moser et al., 2017).

By the end of the second postnatal week (around P15), rat pups open their eyes, gain quadrupedal walking and begin to explore their environment. The first place cells can be identified around P16. They mature gradually reaching adult number and signal around P40. By the end of the third postnatal week (around P20), hippocampus-dependent spatial navigation and spatial learning, as determined by the Morris Water Maze test, emerge (Langston et al., 2010; Wills et al., 2010; Tan et al., 2016).

In this critical period spanning from two to three weeks of age, both CA1 interneurons and pyramidal cells show maturation steps affecting their electrophysiological and biochemical characteristics. On the one hand, parvalbumin-containing GABAergic inhibitory interneurons increased the expression of the channel Kv3.1b, which was associated to shorter APs and could contribute to their fast-spiking activity (Du et al., 1996). On the other hand, CA1 pyramidal cells underwent synaptic and intrinsic plasticities, together with changes in their firing pattern and synaptic connectivity (Hsia et al., 1998; Sánchez-Aguilera et al., 2014, 2017). The current study provides further maturation steps occurring throughout this critical period: changes in the AP morphology of CA1 pyramidal neurons, increase of their excitability and changes in the ion channel expression in the CA1 region.

Taking into consideration the aforementioned, we suggest that maturation of the AP waveform and neuronal excitability described herein could be a consequence of the maturation of visual and motor capacities that take place around P15 (Tan et al., 2016). This could be supported by a previous study, which reported how early eye opening accelerated the development of hippocampus-dependent behavior and excitatory synaptic transmission (Dumas, 2004). Furthermore, we suggest that the currently described developmental changes in CA1 pyramidal neurons could contribute to the

emergence of place cells in the CA1 region from P16 on, and therefore, to the emergence of hippocampus-dependent spatial navigation and spatial learning. The corroboration of this sequence of events (from changes in sensory experience to maturation of CA1 pyramidal neuron intrinsic properties to emergence of place cells and spatial memory) remains as a matter of study for future investigations.

ACKNOWLEDGEMENTS

This research was supported by DGICyT, grant numbers: SAF2007-61361 and SAF2010-20073. A S-A was supported with a Juan de la Cierva Formación Fellowship co-funded by the Spanish Ministry of Science, Innovation and Universities, and the CSIC. We thank Dr. Liset Menéndez de la Prida for her critical review of the manuscript.

REFERENCES

Alfaro-Ruíz R, Aguado C, Martín-Belmonte A, Moreno-Martínez AE, Luján R (2019) Expression, cellular and subcellular localisation of Kv4.2 and Kv4.3 channels in the rodent hippocampus. Int J Mol Sci 20:E246.

Bean BP (2007) The action potential in mammalian central neurons. Nat Rev Neurosci 8:451–465.

Boiko T, Wart A Van, Caldwell JH, Levinson SR, Trimmer JS, Matthews G (2003) Functional specialization of the axon initial segment by isoform-specific sodium channel targeting. J Neurosci 23:2306–2313.

Carter BC, Giessel AJ, Sabatini BL, Bean BP (2012) Transient sodium current at subthreshold voltages: activation by EPSP waveforms. Neuron 75:1081–1093.

Chen S, Yue C, Yaari Y (2005) A transitional period of Ca2+-dependent spike afterdepolarization and bursting in developing rat CA1 pyramidal cells. J Physiol 567:79–93.

Colino A, García-Seoane JJ, Valentín A (1998) Action potential broadening induced by lithium may cause a presynaptic enhancement of excitatory synaptic transmission in neonatal rat hippocampus. Eur J Neurosci 10:2433–2443.

Costa PF (1996) The kinetic parameters of sodium currents in maturing acutely isolated rat hippocampal CA1 neurones. Dev Brain Res 91:29–40.

Costa PF, Ribeiro MA, Santos AI (1991) Afterpotential characteristics and firing patterns in maturing rat hippocampal CA1 neurones in in vitro slices. Dev Brain Res 62:263–272.

Costa PF, Santos AI, Ribeiro MA (1994) Potassium currents in acutely isolated maturing rat hippocampal CA1 neurones. Dev Brain Res 83:216–223.

Debanne D, Campanac E, Bialowas A, Carlier E, Alcaraz G (2011) Axon physiology. Physiol Rev 91:555–602.

Du J, Haak LL, Phillips-Tansey E, Russell JT, McBain CJ (2000) Frequency-dependent regulation of rat hippocampal somato-dendritic excitability by the K + channel subunit Kv2.1. J Physiol 522:19–31.

Du J, Zhang L, Weiser M, Rudy B, Mcbain J (1996) Developmental Expression and Functional Characterization Subunit Kv3.1 b in Parvalbumin-Containing Interneurons of the Rat Hippocampus. J Neurosci 16:506–518.

Dumas TC (2004) Early eyelid opening enhances spontaneous alternation and accelerates the development of perforant path synaptic strength in the hippocampus of juvenile rats. Dev Psychobiol 45:1–9.

Eichenbaum H (2017) Memory: Organization and Control. Annu Rev Psychol 68:19–45.

Giglio AM, Storm JF (2014) Postnatal development of temporal integration, spike timing and spike threshold regulation by a dendrotoxin-sensitive K^+ current in rat CA1 hippocampal cells. Eur J Neurosci 39:12–23.

Gu N, Vervaeke K, Storm JF (2007) BK potassium channels facilitate high-frequency firing and cause early spike frequency adaptation in rat CA1 hippocampal pyramidal cells. J Physiol 580:859–882.

Hsia A, Malenka RC, Nicoll RA (1998) Development of excitatory circuitry in the hippocampus. J Neurophysiol 79:2013–2024.

Hu W, Tian C, Li T, Yang M, Hou H, Shu Y (2009) Distinct contributions of Na(v)1.6 and Na(v)1.2 in action potential initiation and backpropagation. Nat Neurosci 12:996–1002.

Isagai T, Fujimura N, Tanaka E, Yamamoto S, Higashi H (1999) Membrane dysfunction induced by in vitro ischemia in immature rat hippocampal CA1 neurons. J Neurophysiol 81:1866–1871.

Johnston J, Forsythe ID, Kopp-Scheinpflug C (2010) Going native: voltage-gated potassium

channels controlling neuronal excitability. J Physiol 588:3187–3200.

Kim J, Wei D-S, Hoffman DA (2005) Kv4 potassium channel subunits control action potential repolarization and frequency-dependent broadening in rat hippocampal CA1 pyramidal neurones. J Physiol 569:41–57.

Klee R, Ficker E, Heinemann U (1995) Comparison of voltage-dependent potassium currents in rat pyramidal neurons acutely isolated from hippocampal regions CA1 and CA3. J Neurophysiol 74:1982–1995.

Kole MHP, Letzkus JJ, Stuart GJ (2007) Axon initial segment Kv1 channels control axonal action potential waveform and synaptic efficacy. Neuron 55:633–647.

Kuo C, Bean BP (1994) Na+ channels must deactivate to recover from inactivation. Neuron 12:819–829.

Langston R, Ainge J, Couey J, Canto C, Bjerkness T, Witter M, Moser E, Moser M (2010) Development of the spatial representation system in the rat. Science (80-) 328:1576–1580.

Liu PW, Bean BP (2014) Kv2 channel regulation of action potential repolarization and firing patterns in superior cervical ganglion neurons and hippocampal CA1 pyramidal neurons. J Neurosci 34:4991–5002.

Lorincz A, Nusser Z (2008) Cell-type-dependent molecular composition of the axon initial segment. J Neurosci 28:14329–14340.

Lorincz A, Nusser Z (2010) Molecular Identity of Dendritic Voltage-Gated Sodium Channels. Science (80-) 328:906 LP – 909.

Ma M, Koester J (1996) The role of K+ currents in frequency-dependent spike broadening in Aplysia R20 neurons: a dynamic-clamp analysis. J Neurosci 16:4089–4101.

MacDonald SH, Ruth P, Knaus HG, Shipston MJ (2006) Increased large conductance calcium-activated potassium (BK) channel expression accompanied by STREX variant downregulation in the developing mouse CNS. BMC Dev Biol 6:37.

Madeja M (2000) Do neurons have a reserve of sodium channels for the generation of action potentials? A study on acutely isolated CA1 neurons from the guinea-pig hippocampus. Eur J Neurosci 12:1–7.

Martina M, Schultz JH, Ehmke H, Monyer H, Jonas P (1998) Functional and molecular differences

between voltage-gated K+ channels of fast-spiking interneurons and pyramidal neurons of rat hippocampus. J Neurosci 18:8111–8125.

Metz AE, Jarsky T, Martina M, Spruston N (2005) R-type calcium channels contribute to afterdepolarization and bursting in hippocampal CA1 pyramidal neurons. J Neurosci 25:5763–5773.

Mitterdorfer J, Bean BP (2002) Potassium currents during the action potential of hippocampal CA3 neurons. J Neurosci 22:10106–10115.

Moody WJ (1998) Control of spontaneous activity during development. J Neurobiol 37:97–109.

Moser EI, Moser M, McNaughton BL (2017) Spatial representation in the hippocampal formation : a history. Nat Neurosci 20:1448–1464.

Pokorny J, Yamamoto T (1981a) Postnatal ontognesis of hippocampal CA1 area in rats. I. Development of dendritic arborisation in pyramidal neurons. Brain Res Bull 7:113–120.

Pokorny J, Yamamoto T (1981b) Postnatal ontognesis of hippocampal CA1 area in rats. II. Development of ultrastructure in stratum lacunosum and moleculare. Brain Res Bull 7:121–130.

Royeck M, Horstmann MT, Remy S, Reitze M, Yaari Y, Beck H (2008) Role of axonal NaV1.6 sodium channels in action potential initiation of CA1 pyramidal neurons. J Neurophysiol 100:2361–2380.

Rush AM, Dib-hajj SD, Waxman SG (2005) Electrophysiological properties of two axonal sodium channels, Nav1.2 and Nav 1.6 , expressed in mouse spinal sensory neurones. J Physiol 564:803–815.

Sánchez-Aguilera A, Sánchez-Alonso JL, Vicente-Torres MA, Colino A (2014) A novel short-term plasticity of intrinsic excitability in the hippocampal CA1 pyramidal cells. J Physiol 592:2845–2864.

Sánchez-Aguilera A, Sánchez-Alonso JL, Vicente-Torres MÁ, Colino A (2017) Role of low-voltage-activated calcium current and extracellular calcium in controlling the firing pattern of developing CA1 pyramidal neurons. Neuroscience 344:89–101.

Sánchez-Alonso JL, Muñoz-Cuevas J, Vicente-Torres MA, Colino A (2010) Role of low-voltage-activated calcium current on the firing pattern alterations induced by hypothyroidism in the rat hippocampus. Neuroscience 171:993–1005.

Sánchez-Alonso JL, Sánchez-Aguilera A, Vicente-Torres MA, Colino A (2012) Intrinsic excitability is altered by hypothyroidism in the developing hippocampal CA1 pyramidal cells. Neuroscience 207:37–51.

Shao L-R, Halvorsrud R, Borg-Graham L, Storm JF, Fessard IA, Terrasse A De (1999) The role of BK-type Ca2+-dependent K+ channels in spike broadening during repetitive firing in rat hippocampal pyramidal cells. J Physiol 521:135–146.

Shu Y, Hasenstaub A, Duque A, Yu Y, Mccormick DA (2006) Modulation of intracortical synaptic potentials by presynaptic somatic membrane potential. Nature 441:761–765.

Shu Y, Yu Y, Yang J, McCormick DA (2007) Selective control of cortical axonal spikes by a slowly inactivating K+ current. Proc Natl Acad Sci 104:11453–11458.

Spigelman I, Zhang L, Carlen PL (1992) Patch-clamp study of postnatal development of CA1 neurons in rat hippocampal slices: membrane excitability and K+ currents. J Neurophysiol 68:55–69.

Storm JF (1988) Temporal integration by a slowly inactivating K+ current in hippocampal neurons. Nature 336:379–381.

Storm JF (1990) Potassium currents in hippocampal pyramidal cells. In: Understanding the Brain Through the Hippocampus the Hippocampal Region as a Model for Studying Brain Structure and Function (Storm-Mathisen J, Zimmer J, Ottersen OPBT-P in BR, eds), pp 161–187. Elsevier.

Tan HM, Wills TJ, Cacucci F (2016) The development of spatial and memory circuits in the rat. WIREs Cogn Sci 8.

Wang G-Y, Ratto G-M, Bisti S, Chalupa LM (1997) Functional development of intrinsic properties in ganglion cells of the mammalian retina. J Neurophysiol 78:2895–2903.

Wills TJ, Cacucci F, Burgess N, O'Keefe J (2010) Development of the hippocampal cognitive map in preweanling rats. Science 328:1573–1576.

FIGURE LEGENDS

Figure 1: Development of action potential in CA1 pyramidal neurons.

(A) Scheme of the protocol followed: 5 ms threshold depolarizing pulses of intrasomatic current injection were applied at –80 mV to CA1 pyramidal neurons from P9-12 and P16-19 age groups. (B) Representative traces of the APs elicited in neurons from P9-12 (black) and P16-19 (green) age groups. (C) Phase plot that shows the average values of the first derivative of the membrane voltage (dV / dt) versus membrane voltage (V_m) for neurons from P9-12 (black) and P16-19 (green) age groups. The inset shows the repolarizing phase (negative values of dV / dt) at an expanded scale. (D) Box plots representing the median and interquartile range of different AP parameters in neurons from P9-12 (black) and P16-19 (green) age groups. ***P < 0.001. Mann-Whitney U test. $N_{P9-12} = 68$ cells; $N_{P16-19} = 55$ cells.

Figure 2: Subthreshold depolarization (1 s square pulse) differentially modified action potential waveform in developing CA1 pyramidal neurons.

(A) Scheme of the protocol followed: APs were elicited by threshold depolarizing pulses of 5 ms (left) or 1 s (right) duration. The inset shows that 2 APs were fired. In that scenario, we analysed the first AP (red arrow). Scale 20 ms / 20 mV (B) Representative traces of the APs elicited by a threshold pulse of 5 ms (black) or 1 s (red) in neurons from P9-12 (left) and P16-19 (right) age groups. (C) Left: individual values of half-width of APs generated by a threshold pulse of 5 ms (black) or 1 s (red) in neurons from P9-12 (left) and P16-19 (right) age groups. Statistical analysis with Wilcoxon Signed rank test. Right: Box plot representing the median and interquartile range for the half-width of APs elicited by 1 s pulses normalized to those elicited by 5 ms pulses in neurons from P9-12 (black) and P16-19 (green) age groups. Statistical analysis with Mann-Whitney U test (D-F) *Id.* C) for AP repolarization rate, amplitude and overshoot respectively. (G) Left: representative traces of a 1 s threshold pulse that failed to generate an AP in neurons from P9-12 (black) and P16-19 (green) age groups. Right: Box plot representing the median and interquartile range for the peak voltage (left) and the time to reach that potential (right) for P9-12 (black) and P16-19 (green). Statistical analysis with Mann-Whitney U test (H) Left: representative traces of the APs elicited by 1 s threshold pulses in neurons from P9-12 (black) and P16-19 (green) age groups. Right: Box plot representing the median and interquartile range for the AP latency for P9-12 (black) and P16-19 (green) neurons. Statistical analysis with Mann-Whitney U test. ** P < 0.01, ***P < 0.001. $N_{P9-12} = 25$ cells; $N_{P16-19} = 18$ cells.

Figure 3: Subthreshold depolarization (1 s ramp) differentially modified the action potential waveform in developing CA1 pyramidal neurons.

(A) Scheme of the protocol followed: APs were elicited by a 5 ms threshold pulse or by a 1 s depolarizing ramp with threshold intensity. The inset shows that 2 APs were fired. In that scenario, we analysed the first AP (red arrow). Scale 20 ms / 20 mV (B) Representative traces of the APs elicited by a 5 ms pulse (black) or by a 1 s depolarizing ramp (red) in neurons from P9-12 (left) and P16-19 (right) age groups. (C) Left: individual values of half-width of APs generated by a 5 ms pulse (black) or by a 1 s ramp (red) in neurons from P9-12 (left) and P16-19 (right) age groups. Statistical analysis with Wilcoxon Signed rank test. Right: Box plot representing the median and interquartile range for the half-width of APs elicited by 1 s ramps normalized to those elicited by 5 ms pulses in neurons from P9-12 (black) and P16-19 (green) age groups. Statistical analysis with Mann-Whitney U test (D-F) *Id.* C) for AP repolarization rate, amplitude and overshoot respectively. ** $P < 0.01$ ***$P < 0.001$. $N_{P9-12} = 17$ cells; $N_{P16-19} = 14$ cells.

Figure 4: Application of 4-aminopiridine (4-AP) differentially modified AP duration and amplitude in developing CA1 pyramidal neurons.

(A) Representative traces of APs generated by a 5 ms threshold depolarizing pulse before (black) and after (blue) application of 30 µM 4-AP in P9-12 (left) and P16-19 (right) neurons. (B) Left: individual values of the half-width in APs generated by a 5 ms pulse before (black) and after (blue) application of 30 µM 4-AP in neurons from P9-12 (left) and P16-19 (right) age groups. Statistical analysis with Wilcoxon Signed rank test. Right: Box plot representing the median and interquartile range for the AP half-width after application of 30 µM 4AP normalized to control value before drug application in neurons from P9-12 (black) and P16-19 (green) age groups. Statistical analysis with Mann-Whitney U test (C-E) *Id.* B) for AP repolarization rate, amplitude and overshoot respectively. (F-J) *Id*. (A-E) for treatment with 3 mM 4-AP. * $P < 0.05$ ** $P < 0.01$ ***$P < 0.001$. Different sets of neurons were treated with 30 µM 4-AP (A-E: $N_{P9-12} = 12$ cells; $N_{P16-19} = 9$ cells) or 3 mM 4-AP (F-J: $N_{P9-12} = 12$ cells; $N_{P16-19} = 9$ cells).

Figure 5: Expression development of some sodium and potassium channels involved in action potential generation in the CA1 area of the hippocampus.

(A) Upper: individual values of Western blot densitometric analysis showing $Na_v1.2$ expression in the CA1 area of two-week (black) and three-week-old animals (green). Lower: representative Western blot of CA1 membrane extracts. (B-F) *Id.* A) for $Na_v1.6$, $K_v1.2$, BK, $K_v4.2$ and $K_v4.3$ respectively. β-actin was used as loading control. Band density ratios were normalized to β-actin bands. The levels of $Na_v1.2$, $K_v4.2$ and $K_v4.3$ decreased with age and the levels of $Na_v1.6$, $K_v1.2$ and BK channels increased with age in all the independent experiments. N=3 independent experiments for each protein analysed. Comparison between ages with Wilcoxon Signed rank test.

Figure 6: Repetitive firing differentially modified the action potential waveform in developing CA1 pyramidal neurons.

(A) Scheme of the protocol followed: 10 APs were elicited by intrasomatic injection at –80 mV of a train of ten 5 ms current pulses, with enough intensity to elicit one AP in each pulse, at 10 Hz or 50 Hz, in CA1 pyramidal neurons from P9-12 and P16-19 age groups. (B) Representative traces of the APs elicited by the train of ten 5 ms pulses at 10 Hz (up) and 50 Hz (down) in neurons from P9-12 (left) and P16-19 (right) age groups. The first AP is plotted in black, the 2^{nd} to 9^{th} in grey and the tenth in blue. (C) Left: summary graphs representing the median and the interquartile range for the half-width of the APs generated at 10 Hz and 50 Hz (left and right side of the graph, respectively) in both age groups (P9-12: black at 10Hz, grey at 50 Hz; P16-19: dark green at 10 Hz, light green at 50 Hz). Right: *Id*. (Left) for the half-width of successive APs normalized to the half width of the first AP of the train. (D-H) *Id.* (C) for AP repolarization rate, amplitude and overshoot respectively. ***P<0.001 for age factor in a two-way ANOVA. $N_{P9-12} = 16$ cells; $N_{P16-19} = 11$ cells.

Figure 7: Development of CA1 pyramidal neuron excitability.

(A) Representative traces of APs generated by a 1 s current step of 200 pA intensity in neurons from P9-12 (left) and P16-19 (right) age groups. (B) Input-output curve that relates the firing frequency versus intrasomatic current intensity that was injected in neurons from P9-12 (black) and P16-19 (green) age groups. $P < 0.0001$ for age factor in a two-way ANOVA (C) Representative traces of APs generated by a 1 s current step with the intensity required to theoretically depolarize the membrane to a fixed potential (in this case –45 mV) in neurons from P9-12 (left) and P16-19 (right) age groups. (D) Input-output curve that relates the firing frequency versus the theoretical membrane potential that the membrane would have reached according to the Ohm's law in neurons from P9-12

(black) and P16-19 (green) age groups. This input standardization to voltage removes differences mediated by changes in passive properties. $P < 0.0001$ for age factor in a two-way ANOVA (E) Representative traces of the APs elicited by a 1 s current pulse with enough intensity to evoke a maximum firing rate in neurons from P9-12 (left) and P16-19 (right) age groups. (F) Box plot representing the median and interquartile range for the maximum firing rate in neurons from P9-12 (black) and P16-19 (green) age groups. Statistical analysis with Mann-Whitney U test. Comparison between age groups is shown as: ***P<0.001. $N_{P9-12} = 26$ cells; $N_{P16-19} = 18$ cells

FIGURE LEGENDS PRINTED EDITION (NO COLOR)

Figure 1: Development of action potential in CA1 pyramidal neurons.

(A) Scheme of the protocol followed: 5 ms threshold depolarizing pulses of intrasomatic current injection were applied at –80 mV to CA1 pyramidal neurons from P9-12 and P16-19 age groups. (B) Representative traces of the APs elicited in neurons from P9-12 (black) and P16-19 (grey) age groups. (C) Phase plot that shows the average values of the first derivative of the membrane voltage (dV / dt) versus membrane voltage (V_m) for neurons from P9-12 (black) and P16-19 (grey) age groups. The inset shows the repolarizing phase (negative values of dV / dt) at an expanded scale. (D) Box plots representing the median and interquartile range of different AP parameters in neurons from P9-12 (black) and P16-19 (grey) age groups. ***P < 0.001. Mann-Whitney U test. $N_{P9-12} = 68$ cells; $N_{P16-19} = 55$ cells.

Figure 2: Subthreshold depolarization (1 s square pulse) differentially modified action potential waveform in developing CA1 pyramidal neurons.

(A) Scheme of the protocol followed: APs were elicited by threshold depolarizing pulses of 5 ms (left) or 1 s (right) duration. The inset shows that 2 APs were fired. In that scenario, we analysed the first AP (grey arrow). Scale 20 ms / 20 mV (B) Representative traces of the APs elicited by a threshold pulse of 5 ms (black) or 1 s (grey) in neurons from P9-12 (left) and P16-19 (right) age groups. (C) Left: individual values of half-width of APs generated by a threshold pulse of 5 ms (black) or 1 s (grey) in neurons from P9-12 (left) and P16-19 (right) age groups. Statistical analysis

with Wilcoxon Signed rank test. Right: Box plot representing the median and interquartile range for the half-width of APs elicited by 1 s pulses normalized to those elicited by 5 ms pulses in neurons from P9-12 (black) and P16-19 (grey) age groups. Statistical analysis with Mann-Whitney U test (D-F) *Id.* C) for AP repolarization rate, amplitude and overshoot respectively. (G) Left: representative traces of a 1 s threshold pulse that failed to generate an AP in neurons from P9-12 (black) and P16-19 (grey) age groups. Right: Box plot representing the median and interquartile range for the peak voltage (left) and the time to reach that potential (right) for P9-12 (black) and P16-19 (grey). Statistical analysis with Mann-Whitney U test (H) Left: representative traces of the APs elicited by 1 s threshold pulses in neurons from P9-12 (black) and P16-19 (grey) age groups. Right: Box plot representing the median and interquartile range for AP latency for P9-12 (black) and P16-19 (grey) neurons. Statistical analysis with Mann-Whitney U test. ** $P < 0.01$, ***$P < 0.001$. $N_{P9-12} = 25$ cells; $N_{P16-19} = 18$ cells.

Figure 3: Subthreshold depolarization (1 s ramp) differentially modified the action potential waveform in developing CA1 pyramidal neurons.

(A) Scheme of the protocol followed: APs were elicited by a 5 ms threshold pulse or by a 1 s depolarizing ramp with threshold intensity. The inset shows that 2 APs were fired. In that scenario, we analysed the first AP (grey arrow). Scale 20 ms / 20 mV (B) Representative traces of the APs elicited by a 5 ms pulse (black) or by a 1 s depolarizing ramp (grey) in neurons from P9-12 (left) and P16-19 (right) age groups. (C) Left: individual values of half-width of APs generated by a 5 ms pulse (black) or by a 1 s ramp (grey) in neurons from P9-12 (left) and P16-19 (right) age groups. Statistical analysis with Wilcoxon Signed rank test. Right: Box plot representing the median and interquartile range for the half-width of APs elicited by 1 s ramps normalized to those elicited by 5 ms pulses in neurons from P9-12 (black) and P16-19 (grey) age groups. Statistical analysis with Mann-Whitney U test (D-F) *Id.* C) for AP repolarization rate, amplitude and overshoot respectively. ** $P < 0.01$ ***$P < 0.001$. $N_{P9-12} = 17$ cells; $N_{P16-19} = 14$ cells.

Figure 4: Application of 4-aminopiridine (4-AP) differentially modified AP duration and amplitude in developing CA1 pyramidal neurons.

(A) Representative traces of APs generated by a 5 ms threshold depolarizing pulse before (black) and after (grey) application of 30 µM 4-AP in P9-12 (left) and P16-19 (right) neurons. (B) Left:

individual values of the half-width in APs generated by a 5 ms pulse before (black) and after (grey) application of 30 µM 4-AP in neurons from P9-12 (left) and P16-19 (right) age groups. Statistical analysis with Wilcoxon Signed rank test. Right: Box plot representing the median and interquartile range for the AP half-width after application of 30 µM 4AP normalized to control value before drug application in neurons from P9-12 (black) and P16-19 (grey) age groups. Statistical analysis with Mann-Whitney U test (C-E) *Id.* B) for AP repolarization rate, amplitude and overshoot respectively. (F-J) *Id*. (A-E) for treatment with 3 mM 4-AP. * $P < 0.05$ ** $P < 0.01$ ***$P < 0.001$. Different sets of neurons were treated with 30 µM 4-AP (A-E: $N_{P9-12} = 12$ cells; $N_{P16-19} = 9$ cells) or 3 mM 4-AP (F-J: $N_{P9-12} = 12$ cells; $N_{P16-19} = 9$ cells).

Figure 5: Expression development of some sodium and potassium channels involved in action potential generation in the CA1 area of the hippocampus.

(A) Upper: individual values of Western blot densitometric analysis showing $Na_v1.2$ expression in the CA1 area of two-week (black) and three-week-old animals (grey). Lower: representative Western blot of CA1 membrane extracts. (B-F) *Id.* A) for $Na_v1.6$, $K_v1.2$, BK, $K_v4.2$ and $K_v4.3$ respectively. β-actin was used as loading control. Band density ratios were normalized to β-actin bands. The levels of $Na_v1.2$, $K_v4.2$ and $K_v4.3$ decreased with age and the levels of $Na_v1.6$, $K_v1.2$ and BK channels increased with age in all the independent experiments. N=3 independent experiments for each protein analysed. Comparison between ages with Wilcoxon Signed rank test.

Figure 6: Repetitive firing differentially modified the action potential waveform in developing CA1 pyramidal neurons.

(A) Scheme of the protocol followed: 10 APs were elicited by intrasomatic injection at –80 mV of a train of ten 5 ms current pulses, with enough intensity to elicit one AP in each pulse, at 10 Hz or 50 Hz, in CA1 pyramidal neurons from P9-12 and P16-19 age groups. (B) Representative traces of the APs elicited by the train of ten 5 ms pulses at 10 Hz (up) and 50 Hz (down) in neurons from P9-12 (left) and P16-19 (right) age groups. The first AP is plotted in black, the 2^{nd} to 10^{th} in grey. (C) Left: summary graphs representing the median and the interquartile range for the half-width of APs generated at 10 Hz and 50 Hz (left and right side of the graph, respectively) in both age groups (P9-12: black; P16-19: grey). Right: *Id*. (Left) for the half-width of successive APs normalized to the half

width of the first AP of the train. (D-H) *Id.* (C) for AP repolarization rate, amplitude and overshoot respectively. ***P<0.001 for age factor in a two-way ANOVA. N_{P9-12} = 16 cells; N_{P16-19} =11 cells.

Figure 7: Development of CA1 pyramidal neuron excitability.

(A) Representative traces of APs generated by a 1 s current step of 200 pA intensity in neurons from P9-12 (left) and P16-19 (right) age groups. (B) Input-output curve that relates the firing frequency versus intrasomatic current intensity that was injected in neurons from P9-12 (black) and P16-19 (grey) age groups. P < 0.0001 for age factor in a two-way ANOVA (C) Representative traces of APs generated by a 1 s current step with the intensity required to theoretically depolarize the membrane to a fixed potential (in this case –45 mV) in neurons from P9-12 (left) and P16-19 (right) age groups. (D) Input-output curve that relates the firing frequency versus the theoretical membrane potential that the membrane would have reached according to the Ohm's law in neurons from P9-12 (black) and P16-19 (grey) age groups. This input standardization to voltage removes differences mediated by changes in passive properties. P < 0.0001 for age factor in a two-way ANOVA (E) Representative traces of APs elicited by a 1 s current pulse with enough intensity to evoke a maximum firing rate in neurons from P9-12 (left) and P16-19 (right) age groups. (F) Box plot representing the median and interquartile range for the maximum firing rate in neurons from P9-12 (black) and P16-19 (grey) age groups. Statistical analysis with Mann-Whitney U test. Comparison between age groups is shown as: ***P<0.001. N_{P9-12} = 26 cells; N_{P16-19} =18 cells

HIGHLIGHTS

Action potentials in CA1 pyramidal neurons changed from 2 to 3 postnatal weeks

Partial removal of I_A strongly modified the action potential in less mature cells

Expression of $Na_v1.6$, BK and $K_v1.2$ channels increased from 2 to 3 postnatal weeks

Expression of $Na_v1.2$, $K_v4.2$ and $K_v4.3$ channels decreased from 2 to 3 postnatal weeks

Excitability due to active properties increased in these cells from week 2 to week 3